Protein-protein interaction probability landscapes for yeast replicative aging

Hao-Bo Guo[1,2,*] , Weiwei Dang[4] , Hong Qin[1,2,3,*]

[1]Department of Computer Science and Engineering
[2]SimCenter
[3]Department of Biology, Geology and Environmental Science
The University of Tennessee at Chattanooga, Chattanooga, Tennessee 37405, USA
[4]Huffington Center on Aging, Baylor College of Medicine, Houston, Texas 77030, USA

*Correspondence: haobo-guo03@utc.edu and hong-qin@utc.edu

Abstract

We used probability landscapes to map the age-dependent protein-protein interaction profiles during *Saccharomyces cerevisiae* replicative aging. We used quasi-potentials, the negative logarithm of the probabilities, to visualize the downs and rises on the landscapes with respect to the young cells. When the interaction probability is gauged by protein abundance during aging, intra-essential protein interactions fell into a low-potential basin. When the interaction probability is estimated from gene expression, we observed that intra-essential protein interactions were located on a high-potential ridge. These opposite patterns coincide with the previously reported uncoupling of the transcriptome and proteome during yeast aging and were also observed in landscapes on different parameter spaces. A proteome-wide probability landscape revealed that the essential proteins favor the interactions with other essential proteins. The increases in essential hub protein abundances may partly explain the opposite trends observed in the landscapes.

Introduction

The replicative lifespan (RLS) studies in budding yeast, *Saccharomyces cerevisiae*, provided genetic basis of cellular aging from the single cellular organism (McCormick et al. 2015), and contributed to understanding of the aging mechanisms in other organisms including humans (Longo et al. 2012; Wasko and Kaeberlein 2014; Janssens and Veenhoff 2016; Crane and Kaeberlein 2018). Similar to other model organisms such as *Caenorhabditis elegans* (Friedman and Johnson 1988), deletion of a single gene, such as *fob1* in yeast, can significantly extend the lifespan (Defossez et al. 1999). Other factors that affect lifespan, such as caloric restriction (CR), were also found dependent on the genotypes (Schleit et al. 2013). Besides these presumable genetic cues, the individual aging phenotypes vary significantly, even in yeast single cells (Crane and Kaeberlein 2018; Crane et al. 2020). Moreover, the aging phenotypes are dependent on gene expressions. For instance, overexpression of the *sir2* gene could extend the RLS of yeast cells (Kaeberlein and Powers 2007; Guo et al. 2011). A recent work found overexpression of both *sir2* and *hap4* genes leads to a cell state with considerably long RLS (Li et al. 2020).

Whilst the randomness in gene expression, transcription and translation (Raj and van Oudenaarden 2008), enhanced transcriptional fidelity was associated with aging and longevity in yeast (Sen et al. 2015; Ke et al. 2017). The translational efficiencies of different proteins were observed to vary up to hundreds of folds in yeast, however, the variances in both protein and mRNA levels were highly correlated (Lahtvee et al. 2017). Increased noises in both transcriptome and proteome during aging could be part of the cascading events leading to replicative aging and eventual cell death. A recent work

48 reported the proteomics and transcriptomics at different time points along the yeast aging
49 trajectory and identified the "uncoupling" of protein levels to their transcript levels—most
50 notably, of those related to the biogenesis—may be causal of aging (Janssens et al. 2015).
51 It should be noted that the RLS is defined as the total number of daughter cells that a
52 mother cell produced during its life (Longo et al. 2012). In addition, the chronological
53 lifespan, or CLS, is defined as the length of viable time for the yeast cell after being
54 transited into the non-dividing, quiescent state (Longo et al. 2012). The age-dependent
55 data reported by Janssens et al. could be treated as that along the yeast replicative aging
56 (Janssens et al. 2015).

57 It had been widely observed that cell functions arose from the interactions of
58 functional modules (Hartwell et al. 1999). Modularity in interacting protein complexes in
59 the yeast proteome was suggested to be key in the genotype-to-phenotype relationships
60 (Gavin et al. 2006). Based on the age-dependent gene expressions in both fruit-fly and
61 human brain, it was proposed that aging may preferentially attack key regulatory nodes
62 important for the stability of the protein-protein interaction network (PIN) (Xue et al. 2007).
63 Moreover, despite aging does not alter the global and local topologies of the PIN, it is
64 crucial to use the age-specific (or "dynamic") PIN to identify key players in aging (Faisal
65 and Milenkovic 2014).

66 Here, using both the age-dependent transcriptome and proteome data (Janssens
67 et al. 2015), and based on a yeast PIN from a recent update of BioGRID (Oughtred et al.
68 2019) we constructed the Protein-protein Interaction Probability Landscapes (PIPLs).
69 These landscapes treat the young yeast cells (7.8 hr) as the reference, or the "ground
70 state", a term borrowed from the embryonic stem cell (Ying et al. 2008). The old yeast

71 cells ranged from 10.7 to 72.3 hr—i.e., if the ground state was treated as a 10-year-old
72 kid, the aging cells could be considered at ages of 14 to 93 years. In the PIPL, first, all
73 proteins from the PIN were classified into different groups, e.g., based on the RLSs of the
74 single-gene deletion mutants. Then the relative interaction probabilities between different
75 groups of proteins were calculated based on both the protein-protein interaction (PPI)
76 frequencies and the protein concentrations according to the law of mass action. The
77 protein concentrations used here were approximated from either the level of transcripts
78 or proteins in the cell. The interaction probability (p) was then converted to a quasi-
79 potential, $\Delta U = -\log p$, relative to the ground state. Because the relative quasi-potential is
80 additive, those of all protein-protein interactions can be summed up to infer the overall
81 relative quasi-potential between two groups of proteins. Using these relative quasi-
82 potentials, the PIPLs showed valleys and ridges reflecting the high interaction probability
83 basins and low interaction probability barriers, respectively. Note that ΔU is relative to the
84 ground state and the rugged PIPL is shaped by the aging process.

85 The yeast genome has 5,189 verified, 727 uncharacterized and 688 dubious ORFs
86 (as of 8/17/2020) on the *Saccharomyces* Genome Database (Cherry et al. 2012). These
87 ORFs encode ca. 1000 essential genes, with any one of which deleted the cell will not be
88 viable (Ohya et al. 2005; Dowell et al. 2010; Luo et al. 2013; Rancati et al. 2018). It had
89 been suggested that cell death is an emergent phenomenon arising from gradual decay
90 or loss of interactions to essential proteins in the protein-protein interaction network (PIN)
91 (Qin 2019). It had also been suggested that in PIN, the essential proteins are likely to
92 serve as the high-degree hub proteins and vice versa, the hub proteins are likely to be
93 essential, known as the centrality-lethality rule (Jeong et al. 2001). In addition, it had been

shown that the hub proteins (genes) tend to avoid interactions with other hubs, which contribute to the stability of the network (Maslov and Sneppen 2002).

We noticed that gradual variations persisted on the PIPLs along the aging trajectory. However, the PIPLs based on protein abundances differ significantly from those based on the gene expressions, in line with the uncoupling proposed by the previous report (Janssens et al. 2015). For example, whereas based on the proteome the essential versus essential protein interactions fell into a deep basin in the PIPL of old age, based on the transcriptome these interactions were located on a high ridge. To understand the two opposite trends, another proteome-wide landscape was constructed based on comparisons between the empirical PIN and random, null network models (Guo and Qin 2020). In this landscape, we showed that unlike the hub proteins, the essential proteins favor interactions with other essential proteins. We further showed that the abundances of essential hub proteins were significantly increased in aging cells. It is likely the essential hub proteins may account for the discrepancy between the PIPLs from proteome and those from transcriptome.

Result

Aging is characterized by a time-dependent functional decline from birth to death (Lopez-Otin et al. 2013). A recent work reported the proteomics and transcriptomics of the yeast cells at 12 time points along aging, from 7.8 to 72.3 hours (Janssens et al. 2015). Here, we used these age-dependent protein or transcript levels to construct the protein-protein interaction probability landscapes (PIPLs) on dimensions of different parameters.

(a) Landscapes (left) and contours (right) from protein abundance

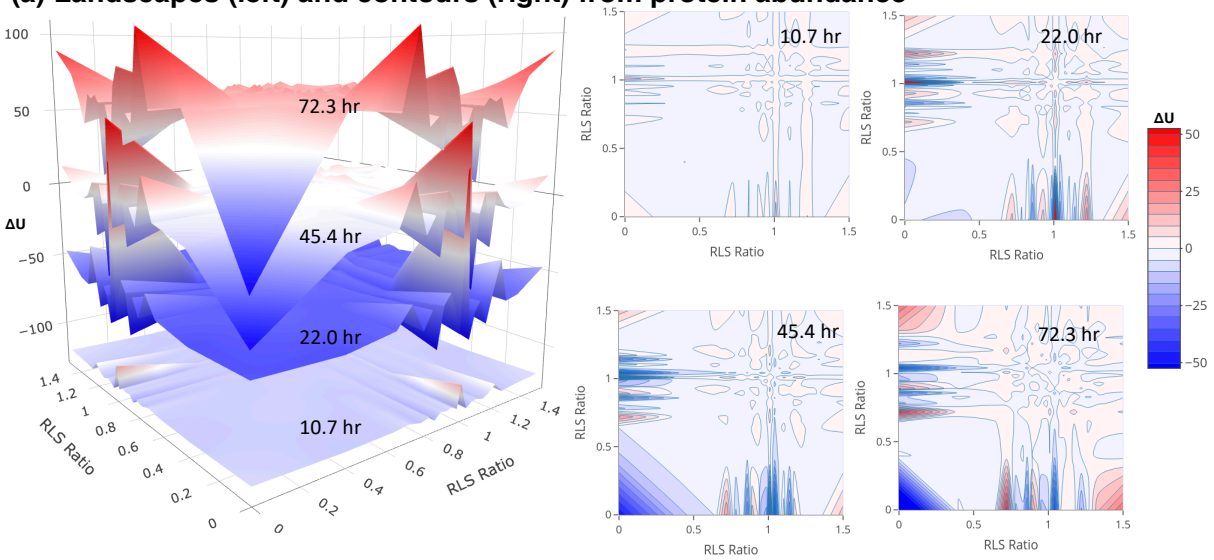

(b) Landscapes (left) and contours (right) from gene expression

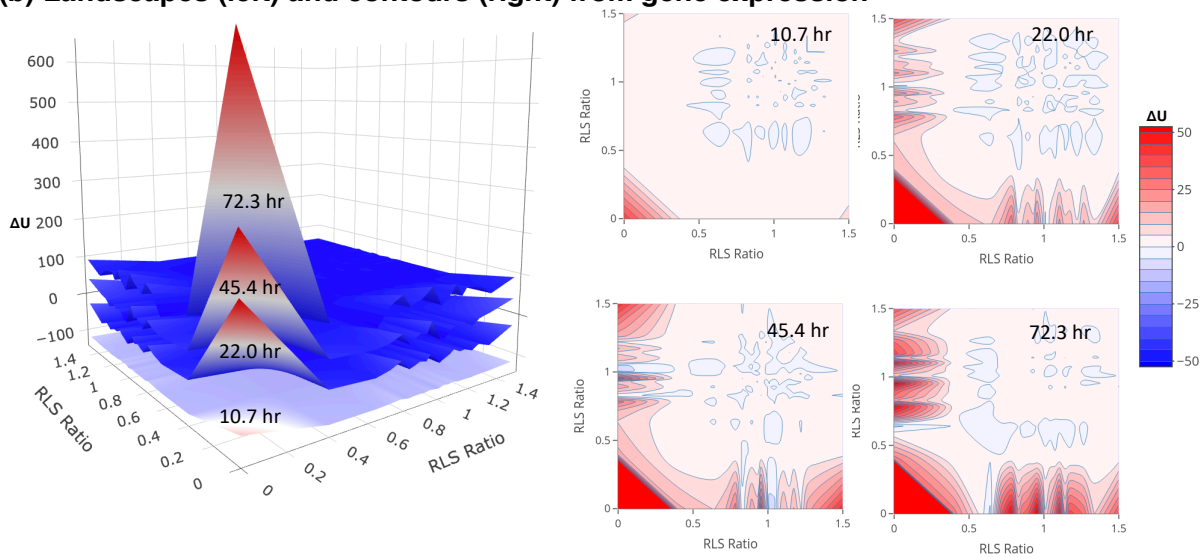

Figure 1. Opposite trends of intra-essential protein interactions during replicative aging as shown by the age-dependent protein-protein interaction probability landscapes (PIPLs) on dimension of RLS ratios. (**a**) Landscapes (left) and contours (right) from protein abundance and (**b**) landscapes (left) and contours (right) from gene expression. The relative quasi potentials (ΔU) were calculated using the youngest cells at 7.8 hr as the reference (ground state). The state parameter of the landscapes is the RLS ratios (or normalized RLS) of the single-gene mutants compared to the WT at the same conditions. The essential genes have RLS ratios of 0. The landscape based on protein abundance shows that the essential-vs-essential interaction region gradually fell into a low-potential basin. However, in the landscape based on gene expression levels the essential-vs-essential interaction region gradually rose up to a high-potential ridge. The landscapes at different ages have been vertically shifted for a better visualization. The color bar shows the relative quasi potentials in the contour maps. A relative color scheme (blue for low and red for high) is applied in landscapes.

132 ***PIPL on RLS and uncoupling of protein abundance and mRNA expression***

133 The age-dependent protein abundance and gene expression had criticized aging
134 as a consequence of uncoupling of protein levels of biogenesis-related genes from the
135 expression levels (Janssens et al. 2015). We constructed the age-dependent PIPLs on
136 dimension of replicative lifespan (RLS) to sample the protein-protein interaction changes
137 associated with the aging process. Here the parameters used are the RLS ratios (or
138 normalized RLS) between the RLS of single-gene deletion mutants and those of the wild
139 type cells cultivated under the same YPD (2% glucose) conditions. The RLS ratios of
140 essential proteins (genes) are 0, as the cell will not be viable after deletion of a single
141 essential gene.

142 Figure 1 shows the landscapes using relative quasi-potentials related to the young
143 cells (i.e., ground state) with the data collected at age of 7.8 hr. Consistent with the
144 observed uncoupling of protein and transcript levels (Janssens et al. 2015), from the
145 PIPLs based on the protein abundance (Figure 1a) and transcription levels (Figure 1b),
146 we also observed a tendency of uncoupling, especially related to the essential proteins.
147 Based on the protein abundances, at the old age, the intra-essential (RLS = 0)
148 interactions fell into a basin, i.e., high interaction probabilities compared to young cells.
149 However, using the expression levels, the intra-essential interactions were located on
150 ridges at the old age, which may be viewed as the potential of loss of interactions within
151 the essential proteins, based on gene expression levels.

(a) Landscapes using RLS and CellSys2017 protein turnover set

Protein abundance-based landscape

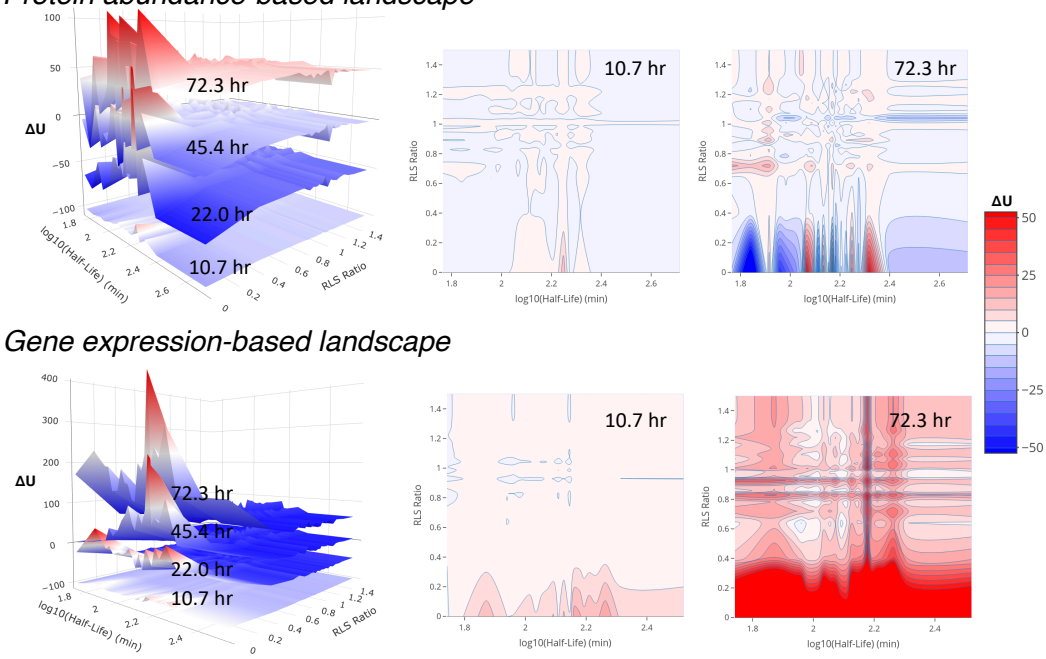

Gene expression-based landscape

(b) Landscapes using RLS and CellRep2014 protein turnover Set

Protein abundance-based landscape

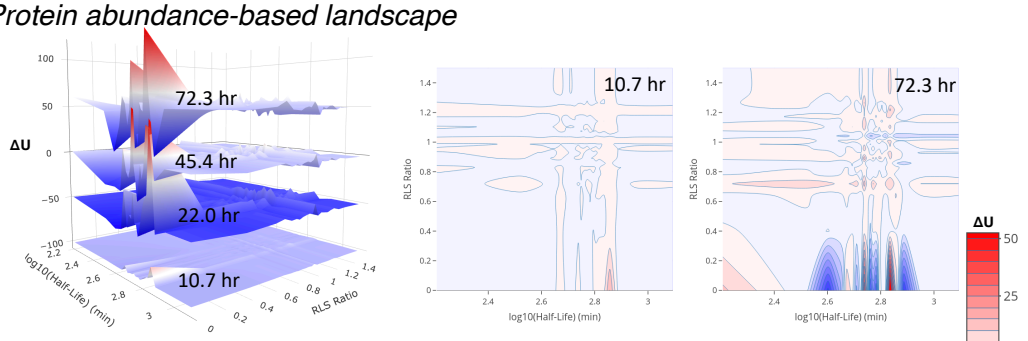

Gene expression-based landscape

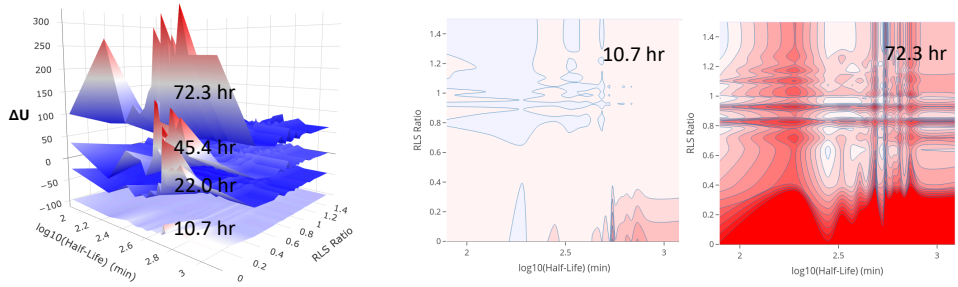

Figure 2. Interactions between essential proteins and short-lived proteins are noisy on the age-dependent PIPLs on dimensions of RLS ratios and protein turnover rates. The protein turnover data were taken from (**a**) the CellSys2017 set and (**b**) the CellRep2014 set, respectively. The landscapes from both sets showed significant differences between the protein-abundance-based (top panels) and gene-expression-based (bottom panels) PIPLs. The contour maps of the landscapes of the aging cells at young (10.7 hr) and old (72.3 hr) are shown for comparisons. The landscapes at different ages have been vertically shifted for a better visualization. The color bar

161 shows the relative quasi potentials in the contour maps. A relative color scheme (blue for low and
162 red for high) is applied in landscapes.

163 ***PIPL on dimensions of RLS versus protein turnover***

164 Two independent protein turnover data sets, the CellSys2017 set (Martin-Perez
165 and Villen 2017) and the CellRep2014 set (Christiano et al. 2014) had been used to
166 construct the age-dependent PIPLs on the dimensions of RLS ratios versus protein
167 turnover rates. Considerable differences can be found between the results of both sets
168 (Figure 2). However, they both interpreted that the short-turnover proteins, which may
169 exhibit higher activities than the long-turnover proteins (Martin-Perez and Villen 2017),
170 had larger fluctuations on the PIPLs of aging cells, especially in interactions with essential
171 proteins. Note that $\log_{10}$-scales had been applied for the turnover rates, in consistent with
172 their distributions (Christiano et al. 2014).

173 Based on the gene expression levels (bottom panels), the landscapes using both
174 turnover sets showed elevated quasi-potentials, especially at old age (Figure 2). However,
175 based on protein abundances, fluctuations of both elevations and declines in the quasi-
176 potentials had been found (Figure 2), consistent with the uncoupling trend between
177 protein and mRNA levels (Janssens et al. 2015). Nevertheless, in all landscapes we
178 observed large fluctuations attributed to the essential genes (RLS ratio of 0) and their
179 interactions with the low-turnover proteins. The interactions between essential genes and
180 high-turnover proteins are relatively stable during aging, according to the protein-
181 abundance-based PIPLs, but not in the gene-expression-based PIPLs.

182 Using the above landscapes, we noted that aging has a higher impact to the gene
183 expressions than to the protein abundances, with respect to the protein-protein
184 interactions. For example, whereas based on the gene expressions for both turnover sets,

185 the interactions with essential genes from all gene groups with different turnovers were in
186 high potential, low probability states, in the protein abundance-based landscapes the
187 interactions between certain groups of genes and the essential genes were dropped to
188 low potential, high probability basins. Moreover, using the CellSys2017 set the low-
189 turnover proteins also showed dropped quasi-potentials or increased interaction
190 probabilities with the essential genes.
191
192 ***PIPL on dimensions of node degrees and RLS ratios***
193 We constructed the PIPL based on the node degrees, as shown in Figure 3a.
194 Based on protein abundances, in the old cells at 72.3 hr, the hub versus hub protein
195 interactions also fell into a basin ($\Delta U = -31$), which was less than the essential versus
196 essential protein interactions ($\Delta U = -83$) shown in Figure 1. The relative quasi-potentials
197 for younger cells were even positive for younger cells from 10.7 to 22 hr (($\Delta U = 0.5$ to 1.8).
198 The extents of the quasi-potentials at other regions were also smaller than those in the
199 PIPL on RLS ratios. For the PIPL based on gene expressions, the interactions with hub
200 proteins, both from other hub and non-hub proteins, generally rose to ridges of the
201 landscape.
202 We also constructed the PIPL based on both the node degrees and RLS ratios
203 (Figure 3b). The interactions between hub and essential proteins of the old cells at 72.3
204 hr fell into a basin with low relative quasi-potential ($\Delta U = -94$). However, those at young
205 age from 10.7 to 26.8 hr were located in ridges, moreover, the hub versus essential
206 interactions in the PIPL at 22.0 hr were on a ridge of $\Delta U = 60$. This analysis indicated that
207 the hub proteins only partly overlap with the essential proteins and vice versa.

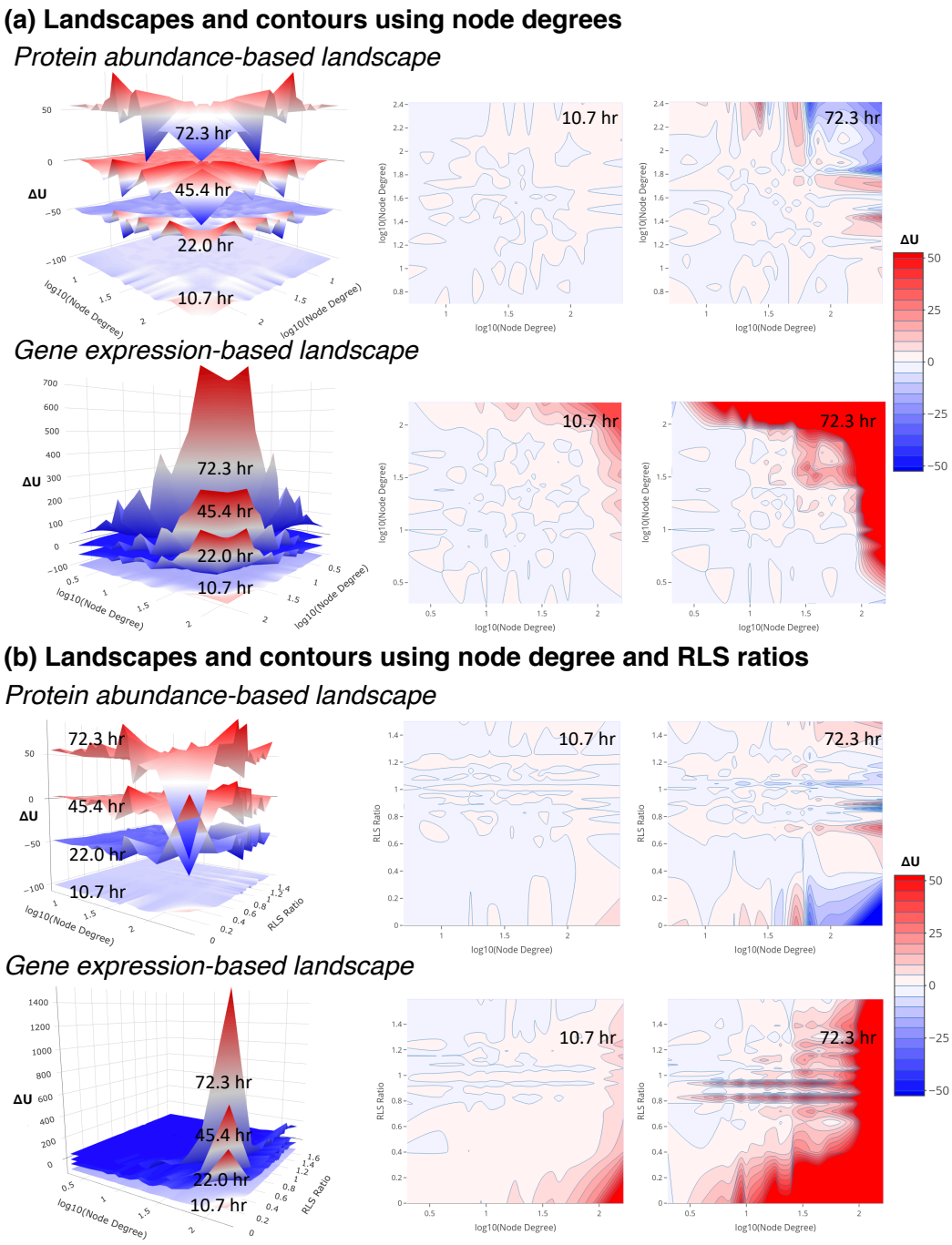

Figure 3. Dissimilarity between the essential and hub proteins from the PIPLs on dimensions of node degrees and RLS ratios. (**a**) PIPLs on node degrees, and (**b**) PIPLs on node degrees versus RLS ratios. The top panels show the PIPLs from protein abundances, and the bottom panels show the PIPLs from transcript abundances. The contour maps of the aging cells at young (10.7 hr) and old (72.3 hr) are shown for comparisons. The landscapes at different ages have been vertically shifted for a better visualization. The color bar shows the relative quasi-potentials in the contour maps. A relative color scheme (blue for low and red for high) is applied in landscapes.

218 ***PIPL on dimensions of RLS versus morphology***

219 A recent work proposed a morphological landscape of yeast aging on which the
220 mother cells took two distinguishable aging paths: in the first path the mother cells
221 produced enlarged and elongated daughter cells, and in the second path the mother cells
222 produced small and round daughter cells (Jin et al. 2019). The mother cells went through
223 the first path had longer RLSs than the mother cells underwent the second path. Two
224 morphologies were used in this landscape to infer the aging paths including the daughter-
225 to-mother size ratios for daughter cell size and the axis ratios of the daughter cells for
226 daughter cell roundness, both at the late stages of cell growths (Jin et al. 2019; Li et al.
227 2020). Here, we combined the RLSs and took advantage of the Saccharomyces
228 Cerevisiae Morphological Database (SCMD2) which recorded 501 morphologies of
229 different yeast single-gene deletion mutants (Saito et al. 2004; Ohya et al. 2005). Figure
230 4 showed both the protein abundance-based and gene expression-based PIPLs of RLS
231 versus morphologies obtained from the SCMD2 including the daughter-to-mother size
232 ratios (C118_C) and daughter axis ratios (C114_C) at the late stages of cell growth from
233 the SCMD, both had been used in the construction of the morphological landscape (Jin
234 et al. 2019).

235

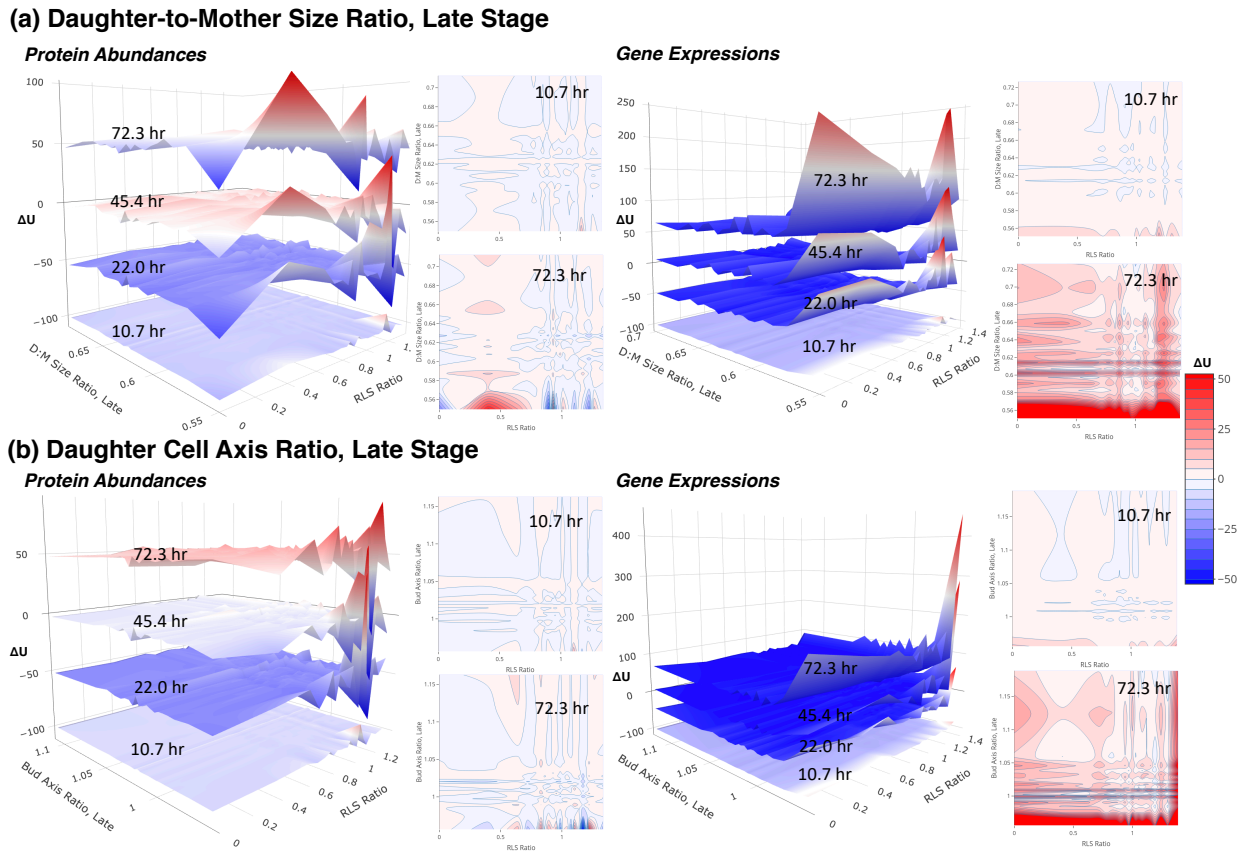

Figure 4. The PIPLs on dimensions of RLS and morphologies. The PIPLs were based on protein abundances (left) or gene expressions (right). The morphologies include (**a**) The daughter-to-mother cell size ratios, and (**b**) the daughter-to-mother cell size ratios. Both morphologies were measured at the late stage of the daughter cell growth, details could be found in the SCMD2 (Ohya et al. 2005). The landscapes at different ages have been vertically shifted for a better visualization. The color bar shows the relative quasi-potentials in the contour maps. A relative color scheme (blue for low and red for high) is applied in landscapes.

Obvious differences between the landscapes based on protein abundances and those based on gene expressions could be found, similar to the landscapes shown above. It should be noted that the morphologies selected from SCMD2 were based on high resolution images of single-gene deletion mutations (Ohya et al. 2005) such that were different than those in the recent morphological landscape (Jin et al. 2019; Li et al. 2020). Moreover, the morphological differences in the early and late stages of the daughter cell growth had also been considered (Ohya et al. 2005). We did observed differences of the absolute values of the morphologies of cells at early growth stage versus those at late

253 growth stage, however, the orders of these genes were not necessarily conserved. These
254 landscapes could therefore be useful to interpret the general trends related to the
255 morphologies. For example, at the old age, the genes related to small daughter cells
256 (Figure 4) seem to have larger fluctuations in the interactions with other proteins.

257 The landscapes from present work described the protein-interaction probabilities
258 (or relative quasi-potentials) of single-gene deletion mutants, and they did not represent
259 cell states. Therefore, these landscapes did not predict how the morphological variations
260 affected the RLS of mother cells as the cell-state landscapes (Jin et al. 2019; Li et al.
261 2020). Instead, the landscapes of present work suggest that the PINs in the old cells had
262 been altered by aging. To rejuvenate to the young cell state, the old yeast cells needed
263 to redistribute the interactions in the PIN, especially from essential genes, to flatten the
264 above age-dependent landscapes.

265

266 ***A proteome-wide protein interaction probability landscape***

267 To further understand why lower relative quasi-potential (or higher probability)
268 have been found in the essential versus essential interactions based on the proteomics,
269 despite the gene expression trend predicted the opposite direction, we constructed
270 another proteome-wide, global landscape model which calculates the probabilities of that
271 the empirical PIN having more interactions than the random null models. As for the age-
272 dependent landscape models, quasi-potentials were calculated as the negative logarithm
273 of the probabilities to infer basins and hills on this landscape. Similar method had been
274 previously applied to a smaller yeast PIN and observed that the high-degree, hub proteins
275 tend to avoid interactions with the other hub proteins, which was suggested to contribute

to the stability of the PIN (Maslov and Sneppen 2002). This approach had been recently applied to estimate the association strengths between different categories of proteins using a human PIN (Guo and Qin 2020). Figure 5 shows the global landscape in the variable spaces of node degrees and RLS ratios of single-gene deletion mutations.

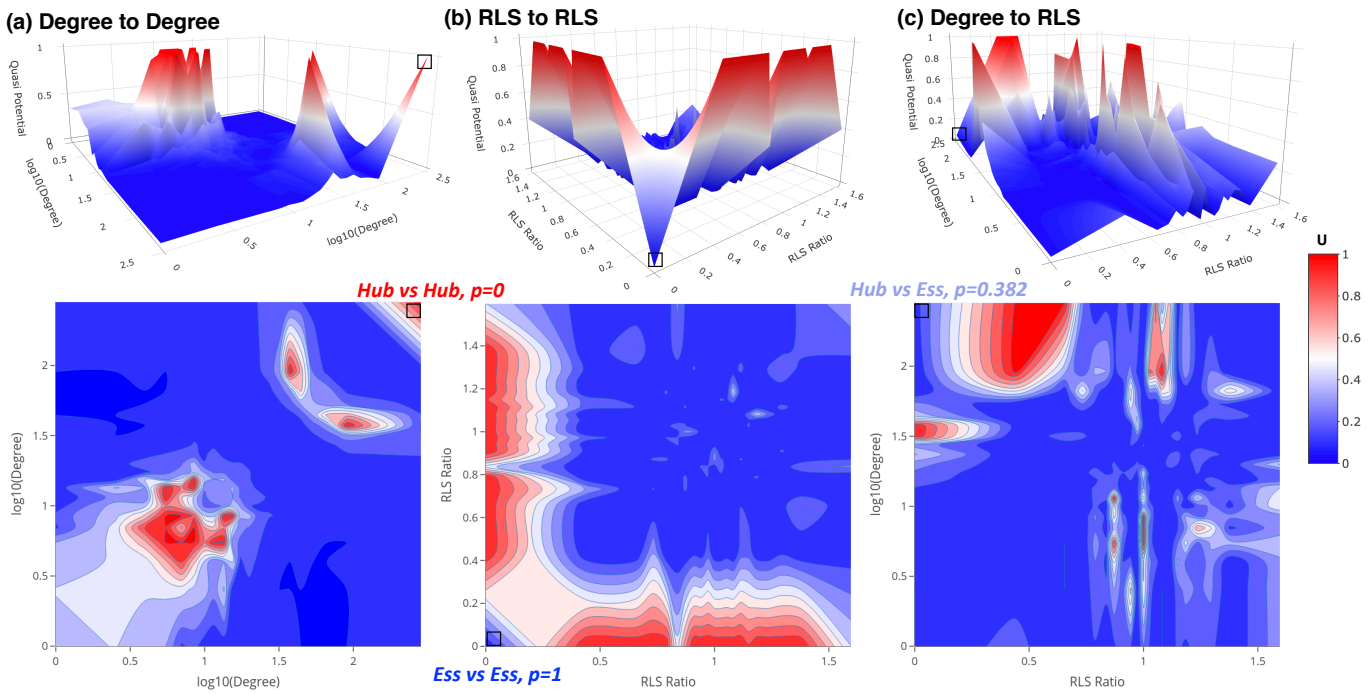

Figure 5. The proteome-wide protein interaction probability landscapes reveal differences between hub and essential proteins. (**a**) The protein interaction landscape on space of the node degrees showed that the hub proteins avoid interactions with other hub proteins (p = 0). (**b**) The essential proteins favor interactions with other essential proteins (p = 1). (**c**) A moderate ratio of hub-essential interactions (p = 0.382) was observed. The hub-hub, essential-essential and hub-essential interaction regions are highlighted as squares on the landscapes and contour maps. The probabilities p indicates the ratio of null network models that showed less interactions than the empirical PIN: p = 1 (such as the essential-essential interactions) indicates the PIN has more interactions than all null models and p = 0 (such as the hub-hub interactions) indicates the PIN has less interactions than all null models, respectively. The quasi potential is calculated as U = $-\log p$, the base of the logarithm function is chosen such that U is in range of [0,1]. 22,188 null network models have been used in this work and the p = 0 (i.e., p < 1/22,188) ratios were converted to p = 1/22,189 for estimation of the quasi potential, U. Top panels show the landscapes and bottom panels show the 2D contour maps. The color bar for both the landscapes and contours are shown at right.

The global landscape on the node-degree space showed that the hub proteins (high-degree proteins in the PIN) tend to avoid interactions with other hub proteins yet

favor the interactions with non-hub proteins (Figure 5a), in agree with previous reports from a smaller yeast PIN (Maslov and Sneppen 2002). Originally observed in yeast PIN, it had been proposed that the hub-proteins in the PIN tend to be essential proteins and vice versa (Jeong et al. 2001). This centrality-lethality rule (or hypothesis) had been confirmed in the PINs of other organisms (Raman et al. 2014) as well as the genetic interaction network (GIN) of yeast (Costanzo et al. 2016). On the global landscape on the RLS space, however, the global landscape indicated that the essential proteins strongly favor the interactions with other essential proteins but tend to avoid the interactions with non-essential proteins (Figure 5b). The probability of the interactions between essential proteins and hub proteins were moderate (Figure 5c). Therefore, the essential proteins and hub proteins should not be treated equally in these landscapes. The above observation might be conflict with the well-known centrality-lethality rule (Jeong et al. 2001; Raman et al. 2014; Peng et al. 2015).

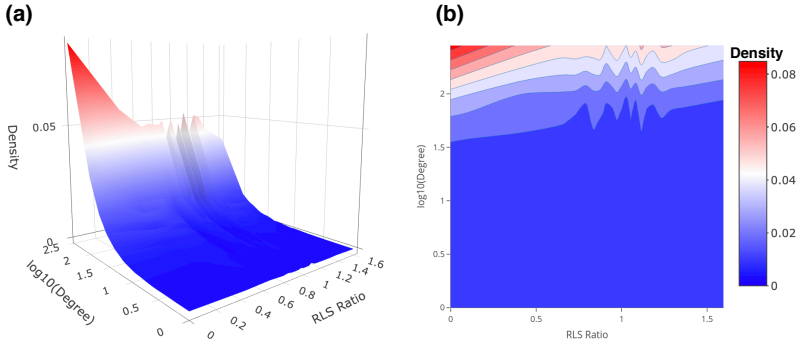

Figure 6. High interaction density was found between essential and hub proteins. The average interaction density calculated on dimensions of node degree and RLS ratios are shown in (**a**) landscape and (**b**) contour map. The interaction density between two sets of nodes is defined as the total number of interactions divided by the by the product of the sizes of both sets.

It is worth noting that the essential genes did have higher degrees (average of 63.3) than non-essential genes (average of 32.7). Based on the landscape on the node degree-

321 RLS space (Figure 5c), we also observed that the interaction densities between hub
322 proteins and essential proteins are significantly stronger than those between the hub
323 proteins and nonessential proteins, also as shown in Figure 6. However, despite of a
324 higher degree in the PIN, a hub protein is not necessarily essential. For example, the
325 most-connected hub protein *dhh1* (YDL160C) has 3,605 interactions in the PIN but is
326 nonessential and the Δ*dhh1* mutant has an RLS ratio of 0.825 compared to the wild type.
327

328 ***Essential hub genes have increased protein abundances in aging cells***

329 We further compared the abundances of 4 categories of proteins (genes) including
330 essential hub, essential non-hub, nonessential hub and nonessential non-hub. The
331 protein or transcript abundances were referenced to the ground state, the young cells
332 with age of 7.8 hr, consistent with the PIPLs shown above. We used the node degree $k \geq$
333 100 as a cutoff (which covered the top 5.8% high connectivity proteins) to classify the hub
334 and non-hub proteins (Figure 7a). The yeast life cycle length of 100 minutes was used to
335 estimate the RLS (Herskowitz 1988). Consistent with the evaluation of the relative-quasi
336 potentials (Methods and Materials), the node degrees were weighted to the protein or
337 transcript abundance values in Figure 7b and 7c. We observed that both the abundances
338 of essential hub proteins increased considerably in the aging cells, however, those of the
339 essential non-hub proteins decreased (Figure 7b). The opposite trends of the average
340 essential protein abundances versus essential transcript abundances (Figure 1) may give
341 an explanation of the differences in the PIPL related to the essential proteins or transcripts.
342 The differences between the average hub proteins and hub transcripts (Figure 3) may
343 also be explained here. We also listed the numbers of proteins (Figure 7b) or transcripts

344 (Figure 7c) that were included in both the PIN the aging proteomics and transcriptomics
345 data set. These trends of protein and/or transcript abundances may partly explain the
346 basins and ridges observed in the protein-protein interaction probability landscapes. Note
347 that the absolute ages of the cells had been approximated to RLSs using an average
348 division time of 100 minutes. This conversion may not be accurate, for example, the actual
349 division time may increase during aging (Jo et al. 2015), and the long estimated RLS in
350 Figure 7 (>30) made it possible that some aging cells may have stopped division and
351 stayed in the post-diauxic, quiescent phase (Longo et al. 2012).

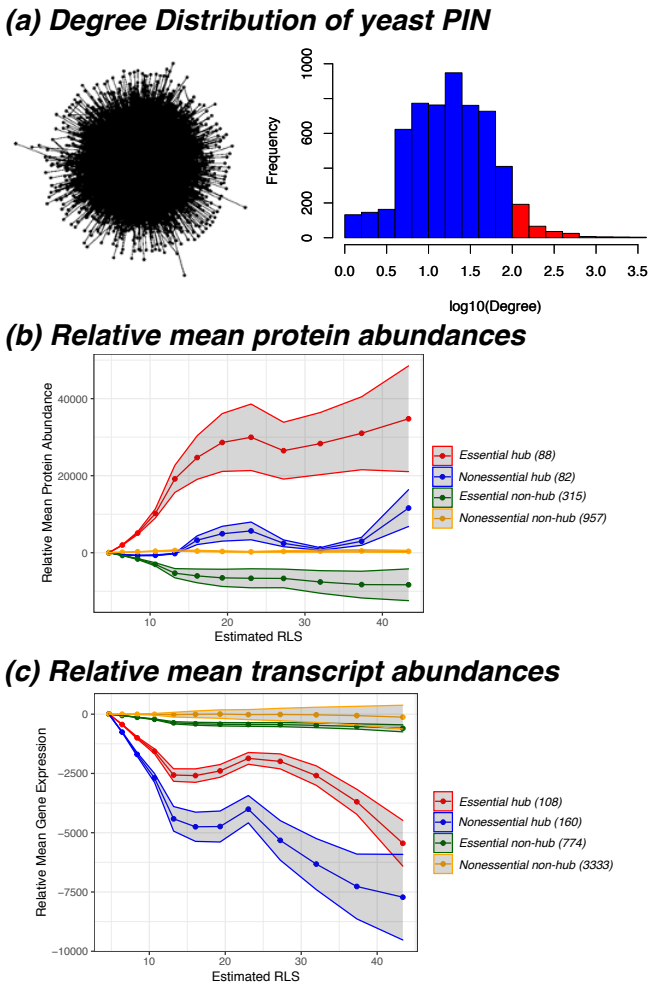

352
353 **Figure 7**. Essential hub proteins (or genes) may account for the opposite trends on the aging
354 landscapes from proteomes and transcriptomes. All proteins (genes) were put in four categories
355 including essential hub (red), nonessential hub (blue), essential non-hub (yellow) and
356 nonessential non-hub proteins or genes. (**a**). Distribution of the node degrees in the yeast PIN. A

snapshot of the PIN was shown at left. The hub proteins (red bars) were selected as the node degree k ≥ 100, which were the top 5.8% high-connectivity proteins of the PIN. (**b**). Relative mean protein abundances. (**c**). Relative mean gene expressions. Average values relative to the young cells at 7.8 hr had been used. The cell ages were approximated to RLS using the dividing time of 100 minutes. The shade of each curve was calculated as the standard deviation from all proteins (genes) of the ratios of aging cells to the ground state, multiplied by the mean differences. The number of proteins (genes) used in the curves of each category had been listed.

Discussion

Present work constructed probability-based protein interaction landscape (PIPL) models. In these age-dependent PIPLs, time-series protein abundance and gene expression data have been adopted to calculate the interaction probabilities between protein groups along aging, and the basins and ridges displayed on the rugged landscape using the young state as the reference, i.e., the relative quasi-potentials, can be regarded as the aging marks. The age-dependent landscapes showed the opposite trends by using the protein abundances versus gene expressions: whereas in the landscapes based on the protein abundances the essential-essential interactions fell into deep basins of low potential or high probability, in the landscapes based on gene expression levels the essential-essential interactions were located to a high potential ridge. The uncoupling between protein abundances and gene expressions had been observed in the original age-dependent proteomic and transcriptomic work and the loss of stoichiometry of protein complexes was suggested to be the consequences of aging (Janssens et al. 2015). This uncoupling may partly explain the opposite trends of the age-dependent landscapes based on proteome versus transcriptome.

The inversed trends between using the protein abundances and gene expressions may be associated with the protein aggregation during the aging process (David et al.

384 2010; Saarikangas and Barral 2015). It may also be owing to the fact that many proteins
385 in yeast have long half-lives (Christiano et al. 2014). A significant amount of proteins
386 underwent non-exponential degradations in the cells and that the protein degradation rate
387 seemed to be age-dependent (McShane et al. 2016). The protein turnover rates were
388 correlated protein functions and activities (Martin-Perez and Villen 2017), and the long-
389 lived proteins may accumulate to high abundances in old cells even though their
390 expression levels had been declined. Using two different protein turnover data sets we
391 further constructed the age-dependent protein interaction landscapes incorporate with the
392 RLS data. In both sets, we observed that based on the protein abundances, the long-
393 turnover proteins exhibited smaller variations than the short-turnover proteins in the old
394 cells referenced to the young cells. However, based on the gene expressions, all proteins
395 show higher quasi potentials for interacting with their partners in the old cells, because of
396 an overall decline of expressions of nearly all genes.

397 Moreover, using a proteome-wide protein interaction landscape, we showed that
398 although protein essentiality was highly associated with its connectivity (the lethality-
399 centrality rule), the high-degree hub proteins tend to avoid the interactions with other hub
400 proteins, whereas the essential proteins favor the interactions with other essential
401 proteins.

402 Loss of proteostasis is a hallmark or a pillar of aging (Lopez-Otin et al. 2013;
403 Kennedy et al. 2014; Sampaio-Marques and Ludovico 2018). The age-dependent protein-
404 interaction landscapes in present work indicate that aging may also cause or be caused
405 by the loss of conservation (or stability) in the protein-protein interaction network, or more
406 generally, in the interactome. We observed that the essential proteins, especially the hub-

407 essential proteins, had the most significant changes in the interacting profiles upon aging.
408 Significant differences had been observed between both the protein abundances and
409 gene expressions of the hub-essential versus hub-nonessential proteins or genes, which
410 may explain the basins at the hub-essential protein regions on the PIPLs based on the
411 protein abundances.

412 Many of the current interests in aging study from model organisms used
413 nonessential genes to understand the genetic basis of aging (Giaever and Nislow 2014;
414 McCormick et al. 2015). From the landscapes presented in present work, it seems that
415 the variations of the protein interaction network may be strongly associated with the
416 essential hub proteins and their interacting partners. If an essential gene had lost all its
417 connections in the PIN, the resulted phenotype may be the same as deletion of this
418 essential gene which would lead to the cell death. Cellular aging can be viewed as
419 emergent property at the gene network level, and the interactions with the essential genes
420 have been suggested to serve as the driver of the aging process (Qin 2019). Therefore,
421 we suggest that the connectivities of essential hub proteins in the PIN may be critical for
422 maintaining the active status of a young, healthy cell.

423 The protein-protein interaction probability landscapes of the budding yeast in
424 present work used the proteomic and transcriptomic data of aging cells mathematically
425 unmixed from bulk cell culture with young daughter cells and dead cells (Janssens et al.
426 2015). We understand that potential biases may persist in the data set and hence in our
427 interpretations. However, using these landscapes we showed that the aging dynamics
428 could be visualized to identify potential aging factors, such as the variations caused by
429 the essential hub proteins. The single cell protein and/or transcript abundance data along

430 aging could be combined with our approach to understand the aging landscape. Moreover,
431 the probability-based interaction landscapes can also be applied using other networks—
432 such as the genetic interaction networks—in understanding of the genotype-phenotype
433 relationships (Costanzo et al. 2016; Costanzo et al. 2019).
434

435 Methods and Materials

436 ***Protein-protein interaction network and random null network models***

437 The empirical protein-protein interaction network (PIN) of S. cerevisiae was
438 obtained from a recent version BioGRID v3.5.177, downloaded on Oct. 1, 2019 (Oughtred
439 et al. 2019). Only the physical interactions related to proteins (excluding the self-
440 interactions) were selected from this PIN, which covers 110,291 edges (interactions)
441 among 5,784 vertices (proteins). The PIN used in present work is regarded as a simple
442 graph, i.e., undirected graph with no self-loops or multi-interactions. 22,188 null network
443 models were built in a way such that all vertices were randomly reshuffled, yet the node
444 degrees preserved as the original PIN. We term these null models the MS02 null models
445 (Maslov and Sneppen 2002; Qin et al. 2003; Guo and Qin 2020).

446 ***Replicative lifespan data***

447 The replicative lifespans (RLSs) of 4,698 single-gene deletion strains of *S.*
448 *cerevisiae* under the YPD (2% glucose) culture had been reported (McCormick et al.
449 2015). In addition, the RLSs of single-gene deletion strains under dietary restriction (DR,
450 0.05% glucose) had been reported (Schleit et al. 2013). 3,939 genes with RLS data under
451 YPD and 342 genes with RLS data under DR were included in the yeast PIN used in

452 present work, providing the opportunity of constructing the protein interaction landscapes
453 of replicative aging.

454 ***Proteomics and transcriptomics data during aging***

455 One set of proteomics and transcriptomics data of *S. cerevisiae* came from a
456 recent report, which comprises the abundances of 1,494 proteins and expression levels
457 of 4,904 genes collected at 12 different ages ranging from 7.8 to 72.3 hours (Janssens
458 et al. 2015). We used the young cells at 7.8 hours as the reference (ground state) to
459 evaluate the PIPLs of the older cells at the other 11 ages.

460 ***Protein turnover time***

461 Two sets of in vivo protein turnover time or half-lives have been used. The
462 CellSys2017 set (Martin-Perez and Villen 2017) comprised of 3,160 proteins with 1,341
463 in the aging proteomics and 2,526 in the aging transcriptomics data sets. The
464 CellRep2014 set (Christiano et al. 2014) included 3,715 proteins with 1,331 in the aging
465 proteomics and 2,988 in the aging transcriptomics data sets.

466 ***Morphologies of single-gene deletion mutants***

467 The morphology data of single-gene deletion mutants were taken from the SCMD2
468 (Saccharomyces cerevisiae morphological database 2) (Ohya et al. 2005). Specifically,
469 two morphologies related to a recent morphological landscape of yeast replicative aging
470 had been analyzed in the protein interaction landscapes (Jin et al. 2019; Li et al. 2020),
471 including the cell size ratio (C118_C) and bud axis ratio (C114_C) at the late stages.
472 Although the definitions of the axis ratio in SCMD2 is different than that used in the
473 morphological landscape, it could provide a rough identification of the roundness of the
474 cell shapes.

475 ***Essential genes of S. cerevisiae***

476 The essential gene set of *S. cerevisiae* were taken from the SCMD2 (Ohya et al.
477 2005) that comprises 1,112 genes, 1,097 of which have interactions recorded in the PIN.

478 ***Selection of gene groups***

479 We used quantiles to catalog the gene groups in the PIPLs. The budding yeast
480 PIN covered 3,939 genes that had the RLS records of the single-gene deletion
481 mutations—the ratios referenced to the control wide type strains had been adopted in the
482 landscapes. The PIN also covered 1,033 essential genes. Among these genes, there
483 were 926 non-essential and 403 essential genes had the age-dependent protein
484 abundance values, and 2,991 non-essential and 882 essential genes had the age-
485 dependent expression values, respectively. In both the age-dependent protein
486 abundance and gene expression sets, the non-essential genes were evenly classified
487 into 20 groups based on the quantiles of the RLS ratios, and the essential genes were
488 classified into one group with the RLS ratio of 0. For the protein node degrees, half-lives
489 and morphology data sets, all genes were classified into 20 quantiles based on the
490 measures. The same classification approach for the RLS groups were applied to the
491 global protein interaction landscape, and all genes included in the PIN and with RLS ratio
492 data had been used.

493 ***Evaluating the quasi-potentials from the landscapes***

494 *Age-dependent protein interaction probability landscape*

495 Aging is a dynamic process reflected in the variations of both protein abundances
496 and gene expressions along the aging process. It had been suggested that a
497 configuration of the cell state could formalized as a vector

$$\mathbf{S_t} = [x_1, x_2, \ldots, x_N]_t, \quad (1)$$

Where N is the total number of genes and x_i is the expression level of the i-th gene (Huang 2009)—we suggest x_i could also be the protein abundance of the i-th protein. Under this definition, the aging process could be regarded as the vector variations along time.

For a simple organism that has two interacting proteins x and y:

$$x + y \xrightarrow{K} xy, \quad (2)$$

the concentration of the complex xy at time t can be calculated as

$$[x]_t[y]_t = K[xy]_t = Kp_t, \quad (3)$$

where K is the equilibrium constant and $[x]_t$ and $[y]_t$ is the concentration of free x and y at time t; i.e., the probability of forming the complex xy at time t, p_t, is approximated as the concentration of [xy] in the cell via equation (3). By using the young cell at time 0 as the reference state or ground state, the equilibrium constant K is canceled out:

$$p_t/p_0 = [xy]_t/[xy]_0 = [x]_t[y]_t/([x]_0[y]_0). \qquad (4)$$

For parameters of all categories of genes—such as the RLSs—a protein-protein interaction probability landscape (PIPL) can be constructed similar to other probability-based cell state Waddington landscapes, which used a quasi-potential, the negative logarithm of the probabilities, to describe the barriers that the cells must overcome for the transition from one attractor state to the other (Huang 2009; Wang et al. 2011). Because all probabilities here are relative to the ground state, the relative quasi potential U_t using U_0 as a reference can be calculated as

$$\Delta U_t = U_t - U_0 = -\log\left(\frac{[xy]_t}{[xy]_0}\right) = -\log\left(\frac{[x]_t}{[x]_0}\right) - \log\left(\frac{[y]_t}{[y]_0}\right). \qquad (5)$$

Equation (5) provides a convenient way to estimate the relative quasi potentials at time t, compared to the young cell ground state.

521 In this work, the relative quasi potential of interactions between two categories of
522 proteins (or genes) are evaluated. The probability is not additive—i.e., we cannot sum up
523 the probabilities of different interactions. However, the logarithm function and hence the
524 quasi potential U is additive. Therefore, it is straightforward to calculate the relative quasi
525 potential of interactions between two sets of genes X and Y based on equation (5). For
526 instance, assuming that there are W interactions between X and Y recorded as (x_i, y_i), i =
527 1, 2, …, W, the relative quasi-potential from all interactions between X and Y would be

528 $$\Delta U_t = -\sum_{i=1}^{W} \log\left(\frac{[x_i]_t}{[x_i]_0}\right) - \sum_{i=1}^{W} \log\left(\frac{[y_i]_t}{[y_i]_0}\right). \quad (6)$$

529 The base of the logarithm function in equation (6) is 10 in present work. It should
530 be noted that in present work all quasi-potentials of every single interaction were relative
531 to the ground state and could therefore bear a value of any real number. The unit of the
532 protein abundances or gene expressions (such as FPKM) were canceled out and did not
533 affect the relative quasi-potentials in equations (4)-(6). In the landscapes of this work, we
534 observed high relative quasi-potentials especially when the interactions between two
535 categories of proteins were dense. However, a cutoff of ±50 was applied in the quasi-
536 potentials of all contour maps because it could capture the indispensable information yet
537 provides relatively good comparison among different landscapes.

538 *Proteome-wide protein-interaction probability landscape*

539 Here we calculated the protein-interaction quasi potentials based on the probability
540 (p) for more interactions between certain categories of genes in the PIN than in the null
541 models. The NetPAS method (Guo and Qin 2020) was used to calculate the p-values
542 using 22,188 null models. The protein-interaction quasi potential U is

543 $$U = -\log p. \quad (7)$$

The base of the logarithm function may vary for the conceptual barriers in equation (7). As 22,188 null models were used, the occurring $p = 0$ cases could be interpreted as $p < 1/22{,}188$, which was converted to $p = 1/22{,}189$ in practice to avoid the infinite log0 values. The resulted quasi-potentials were then normalized to [0,1] for the landscape.

Acknowledgments

This work is supported by NSF Career award #1453078 (transferred to #1720215), BD Spoke #1761839, and internal funding of the University of Tennessee at Chattanooga. All simulations are performed using the SimCenter computing resources of the University of Tennessee at Chattanooga.

Competing Interests

The authors declare no competing interests of this work.

557 # References
558
559 Cherry JM, Hong EL, Amundsen C, Balakrishnan R, Binkley G, Chan ET, Christie KR, Costanzo MC,
560 Dwight SS, Engel SR et al. 2012. Saccharomyces Genome Database: the genomics resource of
561 budding yeast. *Nucleic Acids Res* **40**: D700-705.
562 Christiano R, Nagaraj N, Frohlich F, Walther TC. 2014. Global Proteome Turnover Analyses of the
563 Yeasts S-cerevisiae and S-pombe. *Cell Reports* **9**: 1959-1965.
564 Costanzo M, Kuzmin E, van Leeuwen J, Mair B, Moffat J, Boone C, Andrews B. 2019. Global Genetic
565 Networks and the Genotype-to-Phenotype Relationship. *Cell* **177**: 85-100.
566 Costanzo M, VanderSluis B, Koch EN, Baryshnikova A, Pons C, Tan G, Wang W, Usaj M, Hanchard J,
567 Lee SD. 2016. A global genetic interaction network maps a wiring diagram of cellular function.
568 *Science* **353**: aaf1420.
569 Crane MM, Chen KL, Blue BW, Kaeberlein M. 2020. Trajectories of Aging: How Systems Biology in
570 Yeast Can Illuminate Mechanisms of Personalized Aging. *Proteomics* **20**: 1800420.
571 Crane MM, Kaeberlein M. 2018. The paths of mortality: how understanding the biology of aging can help
572 explain systems behavior of single cells. *Current opinion in systems biology* **8**: 25-31.
573 David DC, Ollikainen N, Trinidad JC, Cary MP, Burlingame AL, Kenyon C. 2010. Widespread Protein
574 Aggregation as an Inherent Part of Aging in C. elegans. *Plos Biology* **8**.
575 Defossez PA, Prusty R, Kaeberlein M, Lin SJ, Ferrigno P, Silver PA, Keil RL, Guarente L. 1999.
576 Elimination of replication block protein Fob1 extends the life span of yeast mother cells. *Mol Cell* **3**:
577 447-455.
578 Dowell RD, Ryan O, Jansen A, Cheung D, Agarwala S, Danford T, Bernstein DA, Rolfe PA, Heisler LE,
579 Chin B et al. 2010. Genotype to Phenotype: A Complex Problem. *Science* **328**: 469-469.
580 Faisal FE, Milenkovic T. 2014. Dynamic networks reveal key players in aging. *Bioinformatics* **30**: 1721-
581 1729.
582 Friedman DB, Johnson TE. 1988. A mutation in the age-1 gene in Caenorhabditis elegans lengthens life
583 and reduces hermaphrodite fertility. *Genetics* **118**: 75-86.
584 Gavin AC, Aloy P, Grandi P, Krause R, Boesche M, Marzioch M, Rau C, Jensen LJ, Bastuck S,
585 Dumpelfeld B et al. 2006. Proteome survey reveals modularity of the yeast cell machinery. *Nature*
586 **440**: 631-636.
587 Giaever G, Nislow C. 2014. The yeast deletion collection: a decade of functional genomics. *Genetics* **197**:
588 451-465.
589 Guo HB, Qin H. 2020. Association study based on topological constraints of protein-protein interaction
590 networks. *Sci Rep* **10**: 10797.
591 Guo ZH, Adomas AB, Jackson ED, Qin H, Townsend JP. 2011. SIR2 and other genes are abundantly
592 expressed in long-lived natural segregants for replicative aging of the budding yeast Saccharomyces
593 cerevisiae. *Fems Yeast Res* **11**: 345-355.
594 Hartwell LH, Hopfield JJ, Leibler S, Murray AW. 1999. From molecular to modular cell biology. *Nature*
595 **402**: C47-C52.
596 Herskowitz I. 1988. Life-Cycle of the Budding Yeast Saccharomyces-Cerevisiae. *Microbiol Rev* **52**: 536-
597 553.
598 Huang S. 2009. Reprogramming cell fates: reconciling rarity with robustness. *Bioessays* **31**: 546-560.
599 Janssens GE, Meinema AC, Gonzalez J, Wolters JC, Schmidt A, Guryev V, Bischoff R, Wit EC,
600 Veenhoff LM, Heinemann M. 2015. Protein biogenesis machinery is a driver of replicative aging in
601 yeast. *Elife* **4**: e08527.
602 Janssens GE, Veenhoff LM. 2016. Evidence for the hallmarks of human aging in replicatively aging
603 yeast. *Microb Cell* **3**: 263-274.
604 Jeong H, Mason SP, Barabasi AL, Oltvai ZN. 2001. Lethality and centrality in protein networks. *Nature*
605 **411**: 41-42.

606 Jin M, Li Y, O'Laughlin R, Bittihn P, Pillus L, Tsimring LS, Hasty J, Hao N. 2019. Divergent Aging of
607 Isogenic Yeast Cells Revealed through Single-Cell Phenotypic Dynamics. *Cell Systems* **8**: 242-253.
608 Jo MC, Liu W, Gu L, Dang WW, Qin LD. 2015. High-throughput analysis of yeast replicative aging
609 using a microfluidic system. *P Natl Acad Sci USA* **112**: 9364-9369.
610 Kaeberlein M, Powers RW. 2007. Sir2 and calorie restriction in yeast: A skeptical perspective. *Ageing*
611 *Res Rev* **6**: 128-140.
612 Ke Z, Mallik P, Johnson AB, Luna F, Nevo E, Zhang ZD, Gladyshev VN, Seluanov A, Gorbunova V.
613 2017. Translation fidelity coevolves with longevity. *Aging Cell* **16**: 988-993.
614 Kennedy BK, Berger SL, Brunet A, Campisi J, Cuervo AM, Epel ES, Franceschi C, Lithgow GJ,
615 Morimoto RI, Pessin JE et al. 2014. Geroscience: Linking Aging to Chronic Disease. *Cell* **159**: 708-
616 712.
617 Lahtvee PJ, Sanchez BJ, Smialowska A, Kasvandik S, Elsemman IE, Gatto F, Nielsen J. 2017. Absolute
618 Quantification of Protein and mRNA Abundances Demonstrate Variability in Gene-Specific
619 Translation Efficiency in Yeast. *Cell Systems* **4**: 495-+.
620 Li Y, Jiang Y, Paxman J, O'Laughlin R, Klepin S, Zhu Y, Pillus L, Tsimring LS, Hasty J, Hao N. 2020. A
621 programmable fate decision landscape underlies single-cell aging in yeast. *Science* **369**: 325-329.
622 Longo VD, Shadel GS, Kaeberlein M, Kennedy B. 2012. Replicative and Chronological Aging in
623 Saccharomyces cerevisiae. *Cell Metabolism* **16**: 18-31.
624 Lopez-Otin C, Blasco MA, Partridge L, Serrano M, Kroemer G. 2013. The Hallmarks of Aging. *Cell* **153**:
625 1194-1217.
626 Luo H, Lin Y, Gao F, Zhang C-T, Zhang R. 2013. DEG 10, an update of the database of essential genes
627 that includes both protein-coding genes and noncoding genomic elements. *Nucleic acids research* **42**:
628 D574-D580.
629 Martin-Perez M, Villen J. 2017. Determinants and Regulation of Protein Turnover in Yeast. *Cell Systems*
630 **5**: 283-+.
631 Maslov S, Sneppen K. 2002. Specificity and stability in topology of protein networks. *Science* **296**: 910-
632 913.
633 McCormick MA, Delaney JR, Tsuchiya M, Tsuchiyama S, Shemorry A, Sim S, Chou AC-Z, Ahmed U,
634 Carr D, Murakami CJ. 2015. A comprehensive analysis of replicative lifespan in 4,698 single-gene
635 deletion strains uncovers conserved mechanisms of aging. *Cell metabolism* **22**: 895-906.
636 McShane E, Sin C, Zauber H, Wells JN, Donnelly N, Wang X, Hou J, Chen W, Storchova Z, Marsh JA et
637 al. 2016. Kinetic Analysis of Protein Stability Reveals Age-Dependent Degradation. *Cell* **167**: 803-
638 815 e821.
639 Ohya Y, Sese J, Yukawa M, Sano F, Nakatani Y, Saito TL, Saka A, Fukuda T, Ishihara S, Oka S et al.
640 2005. High-dimensional and large-scale phenotyping of yeast mutants. *Proc Natl Acad Sci U S A*
641 **102**: 19015-19020.
642 Oughtred R, Stark C, Breitkreutz B-J, Rust J, Boucher L, Chang C, Kolas N, O'Donnell L, Leung G,
643 McAdam R et al. 2019. The BioGRID interaction database: 2019 update. *Nucleic Acids Research* **47**:
644 D529-D541.
645 Peng XQ, Wang JX, Wang J, Wu FX, Pan Y. 2015. Rechecking the Centrality-Lethality Rule in the
646 Scope of Protein Subcellular Localization Interaction Networks. *Plos One* **10**.
647 Qin H. 2019. Estimating network changes from lifespan measurements using a parsimonious gene
648 network model of cellular aging. *Bmc Bioinformatics* **20**.
649 Qin H, Lu HH, Wu WB, Li W-H. 2003. Evolution of the yeast protein interaction network. *Proceedings*
650 *of the National Academy of Sciences* **100**: 12820-12824.
651 Raj A, van Oudenaarden A. 2008. Nature, Nurture, or Chance: Stochastic Gene Expression and Its
652 Consequences. *Cell* **135**: 216-226.
653 Raman K, Damaraju N, Joshi GK. 2014. The organisational structure of protein networks: revisiting the
654 centrality-lethality hypothesis. *Syst Synth Biol* **8**: 73-81.
655 Rancati G, Moffat J, Typas A, Pavelka N. 2018. Emerging and evolving concepts in gene essentiality.
656 *Nature Reviews Genetics* **19**: 34.

657 Saarikangas J, Barral Y. 2015. Protein aggregates are associated with replicative aging without
658 compromising protein quality control. *Elife* **4**.
659 Saito TL, Ohtani M, Sawai H, Sano F, Saka A, Watanabe D, Yukawa M, Ohya Y, Morishita S. 2004.
660 SCMD: Saccharomyces cerevisiae Morphological Database. *Nucleic Acids Research* **32**: D319-
661 D322.
662 Sampaio-Marques B, Ludovico P. 2018. Linking cellular proteostasis to yeast longevity. *Fems Yeast Res*
663 **18**.
664 Schleit J, Johnson SC, Bennett CF, Simko M, Trongtham N, Castanza A, Hsieh EJ, Moller RM, Wasko
665 BM, Delaney JR et al. 2013. Molecular mechanisms underlying genotype-dependent responses to
666 dietary restriction. *Aging Cell* **12**: 1050-1061.
667 Sen P, Dang W, Donahue G, Dai J, Dorsey J, Cao X, Liu W, Cao K, Perry R, Lee JY et al. 2015. H3K36
668 methylation promotes longevity by enhancing transcriptional fidelity. *Genes Dev* **29**: 1362-1376.
669 Wang J, Zhang K, Xu L, Wang E. 2011. Quantifying the Waddington landscape and biological paths for
670 development and differentiation. *P Natl Acad Sci USA* **108**: 8257-8262.
671 Wasko BM, Kaeberlein M. 2014. Yeast replicative aging: a paradigm for defining conserved longevity
672 interventions. *Fems Yeast Res* **14**: 148-159.
673 Xue HL, Xian B, Dong D, Xia K, Zhu SS, Zhang Z, Hou L, Zhang QP, Zhang Y, Han JDJ. 2007. A
674 modular network model of aging. *Molecular Systems Biology* **3**.
675 Ying QL, Wray J, Nichols J, Batlle-Morera L, Doble B, Woodgett J, Cohen P, Smith A. 2008. The
676 ground state of embryonic stem cell self-renewal. *Nature* **453**: 519-U515.
677